Finite-Amplitude Long Waves on Coastal Currents

R. GRIMSHAW AND YI ZENGXIN*

School of Mathematics, University of New South Wales, Kensington, Australia

(Manuscript received 9 March 1989, in final form 12 June 1989)

ABSTRACT

Two models of coastal currents are described that allow fully nonlinear wavelike solutions for the limit of long waves. The first model is an adaptation of a model used by Yi and Warn for finite-amplitude β-plane Rossby waves in a channel. It utilizes a particular choice of continental shelf topography to obtain a nonlinear evolution equation for long waves of finite amplitude. The second model describes the waves that form at the vorticity interface between two regions of constant potential vorticity. Again a nonlinear evolution equation is obtained for long waves of finite amplitude. For both model equations, numerical results are presented and compared with the corresponding results for the BDA equation, which is the weakly nonlinear limit for both models.

1. Introduction

The availability of intensive datasets, obtained both by remote sensing techniques and by the refinement of in situ experimental methods, has resulted in the ability to resolve the structure of flow on the continental shelf and slope on increasingly smaller scales. It now seems clear that coastal currents are often characterized by systems of meanders and "squirts," which sometimes lead to the formation of detached eddies. On the theoretical side, the traditional approach to understanding this phenomena is to study the linearized stability of a model current, which is usually assumed to be uniform in the flow direction. While this approach may well be successful in identifying mechanisms that may initiate meander formation, clearly a nonlinear theory is needed to study the meanders themselves. Of course, techniques for extending linear theory to the weakly nonlinear regime are now well understood (for instance, see Craik 1985 or Pedlosky 1986, for applications in the geophysical fluid dynamics area), although applications to coastal currents are relatively few. However, observed meanders are often of a size which would seem to preclude the direct applicability of a linearized theory, or even a weakly nonlinear theory. Hence it is desirable to attempt to find solutions of the fully nonlinear equations. One option here is to resort, *ab initio,* to numerical methods. An alternative option, and the one we shall pursue here, is to seek finite-amplitude wavelike solutions of the fully nonlinear equations, since this approach has proved fruitful in other physical contexts. In this paper we discuss two models of coastal currents for which we are able to obtain fully nonlinear wavelike solutions in the limit of long waves. Of course, the restriction to long waves precludes a direct application of the present theory to observations since observed meanders typically have longshore scales comparable with the offshore scales. Nevertheless we believe the present study of fully nonlinear long waves is useful for examining finite-amplitude effects and can also serve as a benchmark for (numerical) studies that are not necessarily restricted to long waves.

The first model, discussed in section 2, is an adaptation of a model developed by Warn (1983) and Yi and Warn (1987) for finite-amplitude β-plane Rossby waves propagating on a weak shear flow in a channel. The main new features here are the replacement of the β-plane with the continental shelf waveguide, and the necessity to match the flow on the continental shelf, where the long-wave hypothesis is used, to the flow in the adjoining deep ocean where the flow is nearly in geostrophic balance. The result is a nonlinear evolution equation similar to that obtained by Warn (1983) and Yi and Warn (1987), the principal difference being that the KdV-type dispersive term in their work is replaced here by a dispersive term analogous to that which appears in the evolution equation describing internal solitary waves in a deep fluid (Benjamin 1967 or Davis and Acrivos 1967), denoted in this paper as the BDA equation.

The second model, discussed in section 3, considers waves on the interface between two regions of constant potential vorticity. The analysis is in the spirit of the

* Permanent address: National Research Center for Marine Environment Forecasts, State Oceanic Administration, No. 8 Da Hui Si, Hai Dian Division, Beijing, China.

Corresponding author address: Dr. Roger Grimshaw, School of Mathematics, University of New South Wales, P.O. Box 1, Kensington, New South Wales, Australia 2033

work of Stern (1980), Stern and Pratt (1985) and Pratt and Stern (1986), who studied potential vorticity fronts, but without the effect of bottom topography, which is the main new feature here. Although piecewise constant vorticity models are generally amenable to the powerful techniques of contour dynamics, here we restrict attention to the long-wave limit but impose no a priori restriction on wave amplitudes. The result is a nonlinear equation similar to that obtained in section 2. In particular the dispersive term is again analogous to that which appears in the BDA equation.

In both cases the nonlinear evolution equations that we derive are similar to the KdV, or BDA, equation in that there is a balance between time evolution, nonlinearity and dispersion. We have already noted that the dispersion is of the same kind as that which occurs in the BDA equation. However the present model equations differ significantly from the weakly nonlinear BDA equation in that there is no necessity to introduce a small parameter characterizing the magnitude of the nonlinearity. The model equations discussed here are fully nonlinear, and consequently the nonlinear terms are much more complicated than the simple quadratic term which appears in the BDA equation. For both cases we present some numerical solutions whose main aim is to identify the presence of finite-amplitude waves.

In the remainder of this section we shall present the equations of motion, using the shallow-water nondivergent approximations for barotropic flow. We use nondimensional coordinates based on a horizontal length scale L_1 (typical of the shelf width), a time scale f_1^{-1} where f_1 is the magnitude of the Coriolis parameter, and a vertical length scale h_1 (a typical depth). The nondimensional equations of motion are then

$$\frac{du}{dt} - fv + \zeta_x = 0, \tag{1.1a}$$

$$\frac{dv}{dt} + fu + \zeta_y = 0, \tag{1.1b}$$

$$(hu)_x + (hv)_y = 0, \tag{1.1c}$$

where

$$\frac{d}{dt} = \frac{\partial}{\partial t} + u\frac{\partial}{\partial x} + v\frac{\partial}{\partial y}. \tag{1.1d}$$

Here u, v are the velocity components in the x, y directions respectively and ζ is the sea-surface elevation. The coast is located at $x = 0$, and the ocean depth is $h(x)$ where $h(x)$ is an increasing function of x which tends to h_0 as $x \to \infty$ (see Fig. 1). We shall allow for a possible discontinuity in h at the shelf-break, where h changes abruptly from h_s to h_0. The boundary conditions at such a discontinuity are derived in Appendix A. Elimination of ζ from (1.1a, b) leads to the potential vorticity equation

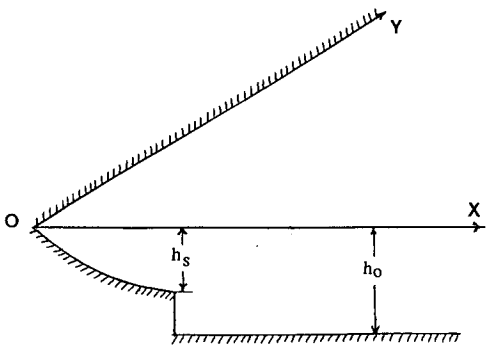

FIG. 1. The coordinate system.

$$\frac{dQ}{dt} = 0, \tag{1.2a}$$

where

$$Q = (\eta + f)/h \tag{1.2b}$$

$$\eta = v_x - u_y. \tag{1.2c}$$

The boundary conditions at the coast, and in the deep ocean, are zero mass flux in the on–offshore direction, so that

$$hu \to 0, \quad \text{as} \quad x \to 0 \tag{1.3a}$$

$$hu \to 0, \quad \text{as} \quad x \to \infty. \tag{1.3b}$$

Next, from (1.1c), we introduce the transport streamfunction ψ,

$$hu = \psi_y, \quad hv = -\psi_x. \tag{1.4}$$

Hence, from (1.2c)

$$\eta = -(\psi_x/h)_x - (\psi_y/h)_y, \tag{1.5}$$

and the potential vorticity equation (1.2a) is an equation for ψ alone. We now replace x with a new variable ξ, where

$$\xi = \int_0^x h(x')dx'. \tag{1.6}$$

Then, from (1.4) and (1.2b) respectively

$$v = -\psi_\xi, \tag{1.7a}$$

$$Q = f/h - \psi_{\xi\xi} - \psi_{yy}/h^2. \tag{1.7b}$$

Also note that the material time derivative (1.1d) is now given by

$$\frac{d}{dt} = \frac{\partial}{\partial t} + \psi_y\frac{\partial}{\partial \xi} - \psi_\xi\frac{\partial}{\partial y}. \tag{1.8}$$

The equation to be solved is thus (1.2a), where Q is given by (1.7b) and d/dt is given by (1.8). The boundary conditions (1.3a, b) become, in terms of ψ,

$$\psi_y = 0, \quad \text{as} \quad \xi \to 0 \tag{1.9a}$$

$$\psi_y = 0, \quad \text{as} \quad \xi \to \infty. \tag{1.9b}$$

2. Waves produced by shear velocity and topographic perturbations

a. Theory

In this section we shall suppose that the ocean region is $\xi > 1$ where $h = h_0$, while the shelf region is $0 < \xi < 1$. Note that the shelf-break is $\xi = 1$ and corresponds to $x = x_s$ where

$$1 = \int_0^{x_s} h(x)dx. \tag{2.1}$$

We shall allow for a discontinuity in depth at $\xi = 1$ so that $h \to h_s$ say as $\xi \to 1-$. It is shown in Appendix A that suitable boundary conditions at $\xi = 1$ are continuity of hu and v, or from (1.4) and (1.7a) respectively,

$$\psi, \psi_\xi \quad \text{continuous at} \quad \xi = 1. \tag{2.2}$$

In the shelf region we let

$$\frac{1}{h(\xi)} = H_0(\xi) + \alpha H(\xi), \tag{2.3a}$$

where

$$H_0(\xi) = D + B\xi. \tag{2.3b}$$

Here α is a small parameter, and so $H(\xi)$ is a topographic perturbation. We shall assume that $H(0) = H(1) = 0$ so that the topographic perturbation is locally confined to the shelf. The choice (2.3b) for the unperturbed topography is made to ensure that the unperturbed equations have a simple solution to the fully nonlinear equations (see subsection 2b). Note that $D + B = h_s^{-1} > 0$, and we must choose $D > 0$, and $B < 0$ in order that $h(\xi)$ is an increasing function of ξ. Further, ignoring the topographic perturbation term $\alpha H(\xi)$ for the moment, we see that the unperturbed depth is $(D^2 + 2Bx)^{-1/2}$ and $x_s = D + \frac{1}{2}B + O(\alpha)$.

We propose to discuss finite-amplitude long waves on a weakly sheared current, in analogy to the theory of Yi and Warn (1987) for Rossby waves on weakly sheared currents. Hence we suppose that

$$\psi \sim -V\xi + \alpha g(\xi), \quad \text{as} \quad y \to -\infty. \tag{2.4}$$

The corresponding longshore current is $V - \alpha g_\xi$ [see (1.2a)], and hence the unperturbed state is a uniform longshore current V, while $g(\xi)$ corresponds to a shear velocity perturbation. We shall suppose that $g(\xi)$ is confined to the shelf zone, so that $g(\xi) \equiv 0$ for $\xi \geq 1$. Further, to ensure that the flow (2.4) satisfies the boundary conditions (1.3a) and (2.2) we must have $g(0) = 0$ and $g(1) = g_\xi(1) = 0$.

Next we anticipate that in the unperturbed flow (i.e., $\alpha = 0$) waves may propagate with a speed c, which we determine in subsection 2b. Hence we write

$$s = y - ct, \tag{2.5}$$

and we also find it convenient to let

$$\psi' = \frac{\psi + c\xi}{c'}, \tag{2.6a}$$

where

$$c' = c - V. \tag{2.6b}$$

Then the condition (2.4) becomes

$$\psi' \sim \xi + \frac{\alpha}{c'} g(\xi), \quad \text{as} \quad s \to -\infty. \tag{2.7}$$

Also the potential vorticity equation (1.2a) becomes, recalling (1.7b) and (1.8)

$$Q_t + c'(\psi'_s Q_\xi - \psi'_\xi Q_s) = 0 \tag{2.8a}$$

where

$$Q = \frac{f}{h} - c'\left(\psi'_{\xi\xi} + \frac{1}{h^2}\psi'_{\xi\xi}\right). \tag{2.8b}$$

To complete the formulation the boundary conditions, (1.9a, b) become

$$\psi' = 0, \quad \text{as} \quad \xi \to 0 \tag{2.9a}$$

$$\psi' \sim \xi, \quad \text{as} \quad \xi \to \infty, \tag{2.9b}$$

while the shelf-break conditions become

$$\psi', \psi'_\xi \quad \text{continuous at} \quad \xi = 1. \tag{2.10}$$

Note that in developing (2.9a, b) from (1.9a, b) we must use the asymptotic condition (2.7).

To describe long waves we now introduce the slow variables

$$\theta = \epsilon s, \quad \tau = \epsilon\alpha t. \tag{2.11}$$

Then (2.8a, b) are replaced by

$$\alpha Q_\tau + c'(\psi'_\theta Q_\xi - \psi'_\xi Q_\theta) = 0 \tag{2.12a}$$

where

$$Q = \frac{f}{h} - c'\left(\psi'_{\xi\xi} + \frac{\epsilon^2}{h^2}\psi'_{\theta\theta}\right). \tag{2.12b}$$

Subsequently we shall show that the appropriate balance between the small parameters ϵ and α is $\alpha = \epsilon$ when h_s/h_0 is O(1), or $\alpha = \epsilon^2$ if h_s/h_0 is $O(\epsilon)$. Also, from the boundary condition (2.9b) it is useful to put

$$\psi' = \xi + \Psi, \tag{2.13a}$$

so that

$$Q = \frac{f}{h} - c'\left(\Psi_{\xi\xi} + \frac{\epsilon^2}{h^2}\Psi_{\theta\theta}\right). \tag{2.13b}$$

The boundary conditions (2.9a, b) become

$$\Psi = 0, \quad \text{as} \quad \xi \to 0, \tag{2.14a}$$

$$\Psi = 0, \quad \text{as} \quad \xi \to \infty. \tag{2.14b}$$

1) OCEAN REGION

This is the region $\xi > 1$ where the depth $h = h_0$. Here the longshore and offshore scales must be identical, and since we have already put $\theta = \epsilon s$ (2.11), we must now put

$$\phi = \epsilon(\xi - 1). \tag{2.15}$$

It then follows from (2.12a, b) and (2.13a, b) that

$$Q = \frac{f}{h_0} + \epsilon^2 Q^{(1)}, \tag{2.16a}$$

where

$$\alpha Q_\tau^{(1)} - c' Q_\theta^{(1)} + \epsilon c'(\Psi_\theta Q_\phi^{(1)} - \Psi_\phi Q_\theta^{(1)}) = 0, \tag{2.16b}$$

$$Q^{(1)} = -c'\left(\Psi_{\phi\phi} + \frac{1}{h_0^2}\Psi_{\theta\theta}\right). \tag{2.16c}$$

Here we recall that $\alpha = \epsilon$ when h_s/h_0 is O(1), or $\alpha = \epsilon^2$ if h_s/h_0 is O(ϵ). We now observe that an exact solution of (2.16b) is $Q^{(1)} = 0$, and this is consistent with the boundary conditions that $\Psi = 0$ as $\phi \to \infty$ (2.14b), and $\Psi = 0$ as $\theta \to -\infty$ [see (2.7) where $g = 0$ for $\xi \geqslant 1$]. Indeed, using this latter boundary condition, (2.16b) implies that $Q^{(1)}$ is O(ϵ), and this result alone would be sufficient for the subsequent analysis. For simplicity we shall work with the stronger hypothesis that $Q^{(1)} = 0$. However, it should be noted that either hypothesis implies that there is a discontinuity in potential vorticity across the shelf-break, and hence the equation for conservation of potential vorticity (1.2a) does not hold at the shelf-break. In Appendix A we show that the boundary conditions at a shelf-break where there is a discontinuity in depth (i.e., $h_0 > h_s$) are (2.10) representing the conservation of onshore mass transport and longshore momentum. It is clear that for $h_0 > h_s$ potential vorticity is not generally simultaneously conserved, and the present approach is most useful when there is a significant discontinuity at the shelf-break. Note that with $Q^{(1)} = 0$, particle paths may cross the shelf-break but their dynamical effect on the ocean is limited. To take full account of the transition from the shelf region to the ocean region requires a more detailed analysis than we can give here, and, in particular, a detailed examination of the transition from the shelf variable ξ to the ocean variable ϕ (2.15). Here, of course, we have assumed that this takes place precisely at the shelf-break, and it is in fact this hypothesis that leads to the conclusion that $Q^{(1)} = 0$. In section 3 we shall consider an alternative model in which the dynamical effect of particle paths crossing the shelf-break is taken more fully into account.

With $Q^{(1)} = 0$, it follows from (2.16c) that

$$\Psi_{\phi\phi} + \frac{1}{h_0^2}\Psi_{\theta\theta} = 0, \quad \text{for} \quad \phi > 0. \tag{2.17}$$

Further, we have already noted that since $g = 0$ in the ocean region it follows from (2.7) and (2.13a) that $\Psi = 0$ as $\theta \to -\infty$. The solution of (2.17), with the boundary condition (2.14b) is now constructed using Fourier transforms. We find that

$$\Psi = \frac{1}{2\pi}\int_{-\infty}^{\infty} \mathcal{F}(\Psi(\phi = 0)) \exp\left(il\theta - \frac{|l|}{h_0}\phi\right) dl, \tag{2.18a}$$

where

$$\mathcal{F}(A) = \int_{-\infty}^{\infty} A(\theta) \exp(-il\theta) d\theta. \tag{2.18b}$$

Here $\mathcal{F}(\cdot)$ is the Fourier transform with respect to θ. Next, using (2.13a) and (2.15) the boundary conditions (2.10) at the shelf-break $\xi = 1$ (i.e., $\phi = 0$) become

$$\Psi_\xi(\xi = 1) = \frac{\epsilon}{h_0}\mathcal{B}(\Psi(\xi = 1)), \tag{2.19a}$$

where

$$\mathcal{B}(A) = -\frac{1}{2\pi}\int_{-\infty}^{\infty} |l| \mathcal{F}(A) \exp(il\theta) dl. \tag{2.19b}$$

Here $\mathcal{B}(\cdot)$ is a pseudodifferential operator and is equivalent to the Hilbert transform which appears in the evolution equation describing internal solitary waves in a deep fluid (Benjamin 1967 or Davis and Acrivos 1967). Note that here we have used the fact that Ψ, Ψ_ξ are continuous at the shelf-break to write (2.19a) in terms of the shelf region solution $\Psi(\xi, \theta, \tau)$. In effect the entire effect of the ocean region on the shelf solution is contained in the boundary condition (2.19a), which thus replaces (2.10).

2) SHELF REGION

This is the region $0 < \xi < 1$ where the governing equations are (2.12a, b), subject to the boundary conditions (2.14a) at $\xi = 0$, (2.19a) at $\xi = 1$ and the asymptotic condition (2.7) as $\theta \to -\infty$. The solution is obtained using the method described by Yi and Warn (1987). Thus we note that

$$\psi'_\theta Q_\xi - \psi'_\xi Q_\theta = -\psi'_\xi\left(\frac{\partial Q}{\partial \theta}\right)_{\psi' = \text{const}}, \tag{2.20a}$$

provided that

$$\psi'_\xi \neq 0. \tag{2.20b}$$

Here the notation indicates that we are taking the derivative of Q with respect to θ while keeping ψ' constant. It follows that (2.12a) becomes

$$Q = \frac{\alpha}{c'}\int_{-\infty}^{\theta}\left(\frac{Q_\tau}{\psi'_\xi}\right)_{\psi' = \text{const}} d\theta' + F(\psi'). \tag{2.21}$$

Here $F(\psi')$ is a function of ψ' alone which is to be

determined by considering the limit $\theta \to -\infty$. Noting (2.3a, b) we put

$$F(\psi') = f(D + B\psi') + \alpha G(\psi'). \quad (2.22)$$

Then taking the limit $\theta \to -\infty$ and using (2.3a, b) and (2.7) we obtain

$$F\left(\xi + \frac{\alpha}{c'} g(\xi)\right) = f(D + B\xi) + \alpha(fH(\xi) - g_{\xi\xi}). \quad (2.23)$$

Comparing (2.22) and (2.23) we can determine $G(\psi')$, and we find that

$$G(\psi') = fH(\psi') - g_{\xi\xi}(\psi') - \frac{fB}{c'} g(\psi') + O(\alpha). \quad (2.24)$$

Recalling (2.13a) we now let

$$\psi' = \psi^{(0)} + \alpha\psi^{(1)} + \cdots, \quad (2.25a)$$

$$\psi^{(0)} = \xi + \Psi^{(0)}. \quad (2.25b)$$

Here we shall adopt the balance $\alpha = \epsilon$ when h_s/h_0 is $O(\epsilon)$. Then from (2.12b), (2.21) and (2.22) we find that

$$c'\Psi_{\xi\xi}^{(0)} + fB\Psi^{(0)} = 0, \quad (2.26a)$$

$$c'\psi_{\xi\xi}^{(1)} + fB\psi^{(1)} = fH(\xi) - G(\xi + \Psi^{(0)}) - \frac{1}{c'}\int_{-\infty}^{\theta} \left(\frac{Q_\tau^{(0)}}{1 + \Psi_\xi^{(0)}}\right)_{\psi^{(0)}=\text{const}} d\theta' - \frac{\epsilon^2}{\alpha} c' H_0{}^2 \Psi_{\theta\theta}^{(0)}, \quad (2.26b)$$

where

$$Q_\tau^{(0)} = -c'\Psi_{\xi\xi\tau}^{(0)}. \quad (2.26c)$$

The boundary conditions (2.14a) and (2.19a) give

$$\Psi^{(0)} = 0, \quad \psi^{(1)} = 0, \quad \text{at} \quad \xi = 0 \quad (2.27a)$$

$$\Psi_\xi^{(0)} = 0, \quad \psi_\xi^{(1)} = \frac{\epsilon}{\alpha h_0} \mathcal{B}(\Psi^{(0)}(\xi = 1)), \quad \text{at} \quad \xi = 1. \quad (2.27b)$$

Also the asymptotic condition (2.7) shows that $\Psi^{(0)} \to 0$ as $\theta \to -\infty$, and $c'\Psi^{(1)} \to g(\xi)$ as $\theta \to -\infty$.

The choice (2.3b) for H_0 was made to ensure that (2.26a) was a linear equation for $\Psi^{(0)}$. With the boundary conditions (2.27a, b) the solution is

$$\Psi^{(0)} = A(\theta, \tau)v(\xi), \quad (2.28a)$$

where

$$v(\xi) = (-1)^n \sin\left(\left(n + \frac{1}{2}\right)\pi\xi\right), \quad (2.28b)$$

$$\frac{fB}{c'} = \left(n + \frac{1}{2}\right)^2 \pi^2, \text{ for } n = 0, 1, 2, \cdots. \quad (2.28c)$$

Thus, as anticipated earlier, the speed c is determined at this stage by (2.28c). Since $B < 0$, $fc' < 0$ and the intrinsic speed c' [see (2.6b)] is negative (positive) in the northern (southern) hemisphere as expected. The amplitude $A(\theta, \tau)$ is undetermined at this stage, and the evolution equation determining A is found by considering the equation (2.26b) and boundary conditions (2.27a, b) for $\psi^{(1)}$. Note that $A \to 0$ as $\theta \to -\infty$, and that the eigenfunction $v(\xi)$ has been normalized so that $v(1) = 1$. Next we put

$$\psi^{(1)} = \Psi^{(1)} + \frac{1}{c'} g(\xi) \quad (2.29)$$

and find that

$$c'\Psi_{\xi\xi}^{(1)} + fB\Psi^{(1)} = N^{(1)}, \quad (2.30a)$$

where

$$N^{(1)} = -G(\xi + Av) + G(\xi) - \frac{1}{c'}\int_{-\infty}^{\theta} \left(\frac{Q_\tau^{(0)}}{1 + Av_\xi}\right)_{\psi^{(0)}=\text{const}} d\theta' - \frac{\epsilon^2 c'}{\alpha} H_0{}^2 v A_{\theta\theta}. \quad (2.30b)$$

Since we are assuming that $g(0) = 0$ and $g(1) = g_\xi(1) = 0$, the boundary conditions (2.27a, b) for $\psi^{(1)}$ apply also to $\Psi^{(1)}$, and $\Psi^{(1)} \to 0$ as $\theta \to -\infty$. The compatibility condition for Eq. (2.30a) is

$$c'[\Psi_\xi{}^{(1)} v - v_\xi \Psi^{(1)}]_0^1 = \int_0^1 N^{(1)} v d\xi. \quad (2.31)$$

This is the required evolution equation for the amplitude $A(\theta, \tau)$. Using the boundary conditions (2.27a, b), (2.28a) and (2.30b) for $N^{(1)}$ we find that (2.31) reduces to

$$\frac{fB}{c'}\int_0^1 v(\xi)d\xi\left\{\int_{-\infty}^{\theta}\left(\frac{A_\tau v}{1 + Av_\xi}\right)_{\psi^{(0)}=\text{const}} d\theta'\right\} + \int_0^1 v(\xi)\{G(\xi + Av) - G(\xi)\}d\xi + \frac{\epsilon c'}{\alpha h_0}\mathcal{B}(A) + \frac{\epsilon^2 c'}{\alpha} A_{\theta\theta}\int_0^1 H_0{}^2 v^2 d\xi = 0. \quad (2.32)$$

The equation (2.32) is similar to that derived by Yi and Warn (1987) in their study of Rossby waves in a shear flow. Indeed, the main differences are that here the eigenfunction v is given by (2.28b) rather than $\sin n\pi\xi$ in Yi and Warn (1987), and here the dispersive term involves the operator $\mathcal{B}(A)$ as well as $A_{\theta\theta}$. We write (2.32) in the form

$$\int_{-\infty}^{\theta} K(A, A')\frac{\partial A'}{\partial \tau} d\theta' + m(A) + \delta\mathcal{B}(A)[+\lambda A_{\theta\theta}] = 0, \quad (2.33)$$

where the kernel $K(A, A')$ is given by

$$K(A, A') = 2\int_0^1 \frac{v(\xi)v(\xi(A', \xi + Av(\xi)))d\xi}{1 + A'v_\xi(\xi(A', \xi + Av(\xi)))}. \tag{2.34}$$

In this expression the equation

$$\psi^{(0)} = \xi + Av(\xi) \tag{2.35}$$

determines $\xi = \xi(A, \psi^{(0)})$ provided that $\psi_\xi^{(0)} \neq 0$ [compare (2.20b)] and hence we must impose the condition $|Av_\xi| < 1$, or

$$|A|\left(n + \frac{1}{2}\right)\pi < 1. \tag{2.36}$$

Following the analysis of Yi and Warn (1987), the expression (2.34) can be written more compactly in the form

$$K(A, A') = 2\int_0^{1+A} \frac{\partial\xi}{\partial A}\frac{\partial\xi}{\partial A'}\,d\psi^{(0)}, \tag{2.37}$$

where here, in the integrand ξ is determined as a function of $A(A')$ and $\psi^{(0)}$ from (2.35), and we recall from (2.28b) that $v(1) = 1$. Next the nonlinear term $m(A)$ and the coefficients δ and λ are given by

$$m(A) = \frac{2}{(n + \frac{1}{2})^2\pi^2}\int_0^1 v(\xi)\{G(\xi + Av) - G(\xi)\}d\xi, \tag{2.38a}$$

$$\delta = \frac{2\epsilon c'}{\alpha h_0(n + \frac{1}{2})^2\pi^2}, \tag{2.38b}$$

$$\lambda = \frac{2\epsilon^2 c'}{\alpha(n + \frac{1}{2})^2\pi^2}\int_0^1 H_0^2 v^2 d\xi. \tag{2.38c}$$

Equation (2.33) is an integro–differential equation for A. The first term represents the evolution of A, the second term is a nonlinear term, and the last two terms represent linear dispersion. When h_s/h_0 is O(1), we choose $\alpha = \epsilon$, and δ is O(1) while λ is O(ϵ). Hence we have placed this term in brackets in (2.33) as it can then be ignored. However, if h_s/h_0 is O(ϵ), we choose $\alpha = \epsilon^2$, and then both δ and λ are O(1), so that both the dispersive terms in (2.33) must be retained. In the limit $A \to 0$ it follows from (2.34) that $K(A, A') \to 1$, and (2.33) becomes an equation of the *KdV*-type. The nonlinear term $m(A)$ is given by (2.38a) and its precise form depends on the choice of $G(\xi)$, which in turn is defined by (2.24). If we suppose, for instance, that

$$g(\xi) = \beta_1\xi(1 - \xi)^2, \quad H(\xi) = \beta_2\xi(1 - \xi), \tag{2.39}$$

then $G(\xi)$ is a cubic polynomial in ξ, and $m(A)$ is a cubic polynomial in A,

$$m(A) = \gamma_1 A + \frac{1}{2}\gamma_2 A^2 + \frac{1}{6}\gamma_3 A^3, \tag{2.40a}$$

where

$$\gamma_1 = \int_0^1 v^2 G_\xi d\xi, \quad \gamma_2 = \int_0^1 v^3 G_{\xi\xi} d\xi, \quad \gamma_3 = \int_0^1 v^4 G_{\xi\xi\xi} d\xi. \tag{2.40b}$$

The coefficients γ_1, γ_2 and γ_3 are readily calculated from (2.24), (2.39) and (2.40b). The linear term in (2.40a) with coefficient γ_1 can be omitted, since a Galilean transformation $\theta \to \theta - \gamma_1\tau$ will remove it. To show this we must use the identity

$$\int_{-\infty}^{\theta} K(A, A')\frac{\partial A'}{\partial\theta'}\,d\theta' = A, \tag{2.41}$$

which may be readily established from (2.37).

Steady solitary wave solutions of (2.33) have the form $A(\hat\theta)$, where $\hat\theta = \theta - w\tau$ and w is the wave speed, or more precisely αw is the correction to the basic speed c. Substitution into (2.33), and utilization of (2.41), then gives

$$-wA + m(A) + \delta\mathcal{B}(A)[+\gamma A_{\hat\theta\hat\theta}] = 0. \tag{2.42}$$

For the case $\delta = 0$, the solitary wave solutions of (2.42) have been discussed by Warn (1983). For the particular case when $m(A)$ is given by the cubic polynomial (2.40a), it reduces to the integrated form of the modified *KdV* equation, which has the solitary wave solution (see Kabutani and Yamasaki 1978 or Miles 1979)

$$A = \frac{a\,\mathrm{sech}^2(\hat\theta/\beta)}{1 - b\tanh^2(\hat\theta/\beta)}, \tag{2.43a}$$

where

$$w - \gamma_1 = \frac{1}{3}\gamma_2 a + \frac{1}{12}\gamma_3 a^2 = \frac{4\lambda}{\beta^2}, \tag{2.43b}$$

$$\frac{4\lambda}{\beta^2}(1 - b) = \frac{1}{3}\gamma_2 a + \frac{1}{6}\gamma_3 a^2. \tag{2.43c}$$

For the solutions to be bounded, $b < 1$, which implies that either $\gamma_3 a/\gamma_2 > -2$ or $\gamma_3 a/\gamma_2 < -4$. Of course, when $\gamma_3 = 0$, $b = 0$ and (2.43a–c) reduce to the well-known "sech^2"-solitary wave solution of the *KdV* equation. It is also of interest to note that when $\lambda\gamma_3 < 0$, there exist borelike solutions,

$$A = -\frac{\gamma_2}{\gamma_3}\{1 \pm \tanh(\hat\theta/\beta)\}, \tag{2.44a}$$

where

$$w - \gamma_1 = -\frac{\gamma_2^2}{3\gamma_3} = \frac{4\lambda}{\beta^2}, \tag{2.44b}$$

which correspond to the limit $b \to 1$ in (2.43b, c).

On the other hand, when $\lambda = 0$ and $m(A)$ is given by (2.40a) with $\gamma_3 = 0$, Eq. (2.42) reduces to an integrated form of the equation which describes internal

solitary waves in deep fluids (Benjamin 1967 or Davis and Acrivos 1967), which we shall call the BDA equation. It has the solitary wave solution

$$A = \frac{a}{1 + (\hat{\theta}/\beta)^2}, \tag{2.45a}$$

where

$$w - \gamma_1 = \frac{1}{4}\gamma_2 a = \frac{\delta}{\beta}. \tag{2.45b}$$

However, when $\gamma_3 \neq 0$, or $m(A)$ is given by some other nonlinear expression than (2.40a), explicit solitary wave solutions of (2.40a) do not appear to be known. A similar situation exists when δ and λ are both nonzero, although when $m(A)$ is given by (2.40a) with $\gamma_3 = 0$, we have found the solitary wave solution

$$A = a\left\{\frac{1}{1 + (\hat{\theta}/\beta)^2} + \frac{\sigma}{(1 + (\hat{\theta}/\beta)^2)^2}\right\} \tag{2.46a}$$

where

$$w - \gamma_1 = \frac{5a}{48}\gamma_2(2 + \sigma)^2 = \frac{\delta}{\beta}\left(1 + \frac{1}{2}\sigma\right), \tag{2.46b}$$

$$\frac{\delta}{\beta} = 5\frac{\lambda}{\beta^2}\left(1 + \frac{2}{\sigma}\right), \tag{2.46c}$$

$$\sigma = \frac{2}{\sqrt{5}}\left\{\left(\frac{\sqrt{5}+1}{2}\right)^{1/3} + \left(\frac{\sqrt{5}-1}{2}\right)^{1/3}\right\} \approx 1.812\cdots. \tag{2.46d}$$

However, this solution is just a curiosity as it is isolated in parameter space, since (2.46c) shows that β (and hence w, a) must take a unique value.

b. Numerical results

The equation to be solved is (2.33), where we now assume that $m(A)$ is given by (2.40a) with $\gamma_1 = 0$. As it stands (2.33) can be regarded as a Volterra integral equation of the first kind for $\partial A/\partial\tau$. The numerical solution of such integral equations is generally ill-posed, and hence, as in Yi and Warn (1987), we convert (2.33) to an integral equation of the second kind by differentiation with respect to θ. The result is

$$A_\tau + A_\theta \int_{-\infty}^{\theta} \hat{K}(A, A')\frac{\partial A'}{\partial \tau}\, d\theta' + \frac{1}{K(A, A)}\{m'(A)A_\theta + \delta\mathcal{B}(A_\theta) + [\lambda A_{\theta\theta\theta}]\} = 0 \tag{2.47a}$$

where

$$\hat{K}(A, A') = \frac{K_A(A, A')}{K(A, A)}. \tag{2.47b}$$

The numerical procedure for solving (2.47a) is a pseudospectral method of a kind developed by Fornberg and Whitham (1978) for equations of the KdV-type. The novel feature here is the integral term. The method of treating this term, and other details of the numerical scheme are analogous to those used by Yi and Warn (1987) for a similar equation, and we refer the reader to this publication for further information.

In the small-amplitude limit $A \to 0$, $K(A, A') \to 1$ and (2.42a) reduces to

$$A_\tau + \gamma_2 A A_\theta + \delta\mathcal{B}(A_\theta) + [\lambda A_{\theta\theta\theta}] = 0. \tag{2.48}$$

When the term $[\lambda A_{\theta\theta\theta}]$ is omitted, (2.48) is the BDA equation. On the other hand, when $\delta = 0$ (i.e., $h_0 \to \infty$) and the term $[\lambda A_{\theta\theta\theta}]$ is retained it is the KdV equation. Thus, the equation (2.47a) can be regarded as a higher-order nonlinear extension of either of these canonical equations, and it is from this point of view that we shall present our numerical results. Since the integral equation discussed by Yi and Warn (1987) corresponds to the case $\delta = 0$, here we shall concentrate on the opposite case when the term $[\lambda A_{\theta\theta\theta}]$ is omitted (i.e., we set $\lambda = 0$), but δ is nonzero.

In choosing numerical values for the constants δ, γ_2, γ_3 and λ, we note that the first two are disposable since a rescaling of the variables τ and θ allows both to be chosen arbitrarily. If $\delta\gamma_2 > 0$ (<0) the sign of θ is preserved (changed), while the sign of τ is, of necessity, preserved. Note also that δ has the same sign as c' [see (2.38b) where c' is positive in a Southern Hemisphere scenario, see (2.28c)]. Here we shall put $\delta = 2.5$, $\gamma_2 = 10$ and vary the remaining parameters, γ_3 and λ. Also we shall only consider the fundamental mode $n = 0$ [see (2.28b)]. For the initial condition we choose

$$A(\tau = 0) = \frac{a_0}{1 + \{(\theta - \theta_0)/\beta_0\}^2}. \tag{2.49}$$

Varying the parameters a_0 and β_0 allows us to generate a variety of solutions. It is pertinent here to recall the condition (2.36) which, with $n = 0$, implies that we must choose a_0 so that $|a_0| < 2/\pi$. The parameter θ_0 simply determines the origin for the θ-coordinate, and in each case is chosen to fit the maximum information into the computational domain.

At first we choose $\gamma_3 = 0$ and $\lambda = 0$, and, as discussed above we shall always put $\gamma_1 = 0$. We have already shown that for this parameter setting, the BDA solitary wave (2.45a, b) is a solution of (2.47a), as well as being a solution of the BDA equation (2.48). Hence interest for this case centers on the time evolution of the solutions of the fully nonlinear equation when compared with the small-amplitude limit (2.48). We put $\beta_0 = 10$ and consider the numerical integration of (2.47a) for a range of values of a_0 from 0.1 to 0.5. First, we note that when $a_0 = 0.1$, $a_0\beta_0 = 4\delta/\gamma_2 = 1$, thus satisfying the condition for a solitary wave solution (2.45a, b). For this case, the numerical integration in-

deed produced a single solitary wave. A typical result for other values of a_0 is shown in Fig. 2 for $a_0 = 0.3$. We see that a well-defined wave has emerged, accompanied by the formation of a secondary wave; although it cannot be seen on the scale of the figure, a third wave has also formed, together with some trailing oscillations. These features are qualitatively similar to the behavior to be expected from the BDA equation (2.48), which for this particular initial condition, would be expected to produce three solitary waves. It is pertinent to note here that for the BDA equation (2.43) the choice of a_0 is immaterial provided that $a_0\beta_0$ is fixed, since a rescaling of A allows a_0 to be chosen arbitrarily. However, this is not possible for the fully nonlinear equation (2.47a). While the time evolution of the wave field is analogous to that of the BDA equation (2.48), a major difference is the presence of the constraint (2.36) (here with $n = 0$) for the fully nonlinear equation (2.47a). For the case $a_0 = 0.2$, the numerical results indicate that the constraint is satisfied for all times $\tau \geqslant 0$. However, for $a_0 = 0.3$, the constraint is violated at $\tau = \tau_c$, where $\tau_c \approx 37$; further as a_0 is increased, τ_c is decreased. Once τ_c is reached, the numerical integration cannot be continued further, and hence for these cases, the final form of the wave field cannot be determined. We recall that the constraint (2.36) is due to the requirement (2.20b) that $\psi'_\xi \neq 0$, or more precisely $\psi'_\xi > 0$. Recalling (1.7a) and (2.6a), and that here c' is positive, we see that the constraint is equivalent to $v < c$, where we recall that v is the longshore velocity, and c is the wave speed defined by (2.6b) and (2.28c). Thus the constraint, in a frame of reference moving with speed c, is equivalent to the requirement that the relative longshore velocity should be negative, and hence excludes the presence of regions of reversed flow. It would be tempting to conclude that the constraint can be interpreted as a criterion for wave breakdown. However, we adopt the more cautious view that the constraint is a consequence of our formulation of the problem, and that waves with regions of reversed flow are not automatically excluded.

Next, we retain the conditions $\gamma_3 = 0$ and $\lambda = 0$, and again use the initial condition (2.49), but now choose $a_0 < 0$. A typical result is shown in Fig. 3 for $a_0 = -0.3$ and $\beta_0 = 10$. With the exception of the sign of a_0, the parameter setting is the same as that for Fig. 2. However, the wave field now consists of an oscillatory wavetrain propagating in the negative θ-direction. Again these features are typical of the behavior to be expected from the BDA equation (2.48), which for this negative initial condition would produce a similar trailing oscillatory wavetrain.

Let us now turn to the case when γ_3 is not zero, although we still put $\lambda = 0$. Note that for the illustrative examples (2.39), γ_3 is zero for a purely topographic perturbation (i.e., $\beta_1 = 0$, but $\beta_2 \neq 0$); otherwise γ_3 will generally be of comparable magnitude to γ_2. Here we put $\gamma_3 = \pm 20$ so that $|\gamma_3| = 2\gamma_2$. Typical results for these two cases are shown in Figs. 4a, b, where we have again used the initial condition (2.49); the results shown are for $a_0 = 0.2$ and $\beta_0 = 10$. Referring to equation (2.47a), where $m'(A)$ is obtained from (2.40a), we see that the effect of the parameter γ_3 on the nonlinear term $m'(A)A_\theta$ is to replace the term $\gamma_2 AA_\theta$ with $(\gamma_2 + \frac{1}{2}\gamma_3 A)AA_\theta$. Thus, with our positive initial condition, we would expect the case $\gamma_3 = 20$ (-20) to resemble the corresponding case for $\gamma_3 = 0$ but with an increase (decrease) of the effects of nonlinearity. This is apparent in Figs. 4a, b, since in Fig. 4a for $\gamma_3 = 20$ a secondary wave can be seen in addition to the main well-defined wave, a feature which is not apparent in Fig. 4b for $\gamma_3 = -20$. Also the main wave is higher and steeper for $\gamma_3 = 20$ compared to $\gamma_3 = -20$. In both cases the general features are comparable with the case $\gamma_3 = 0$ (see Fig. 2) when due account is taken of the increase (decrease) of the effects of nonlinearity.

Finally, in our discussion of (2.47a), we consider the effect of allowing the coefficient λ to be non-zero, in order to consider the influence of KdV-type dispersion vis-a-vis that of BDA-dispersion. We set $\gamma_3 = 0$ and $\lambda = 2.5$, with δ and γ_2 retaining the values set previously. We again use the initial condition (2.49),

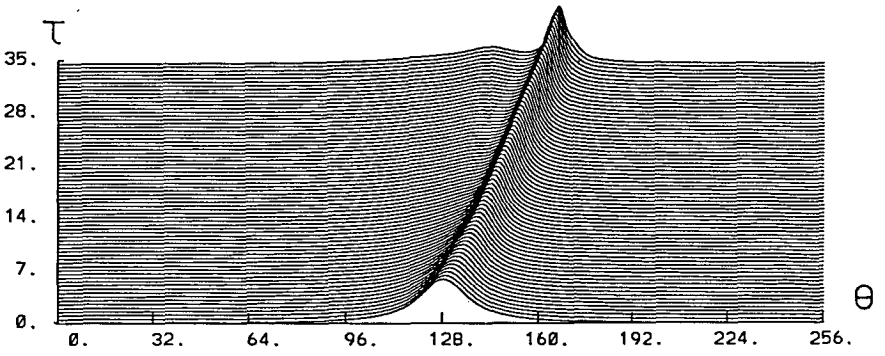

FIG. 2. Results for the numerical integration of the nonlinear evolution equation (2.47a). The parameter setting is $\delta = 2.5$, $\lambda = 0$, $\gamma_2 = 10$, $\gamma_3 = 0$. The initial condition is (2.49) with $a_0 = 0.3$ and $\beta_0 = 10$.

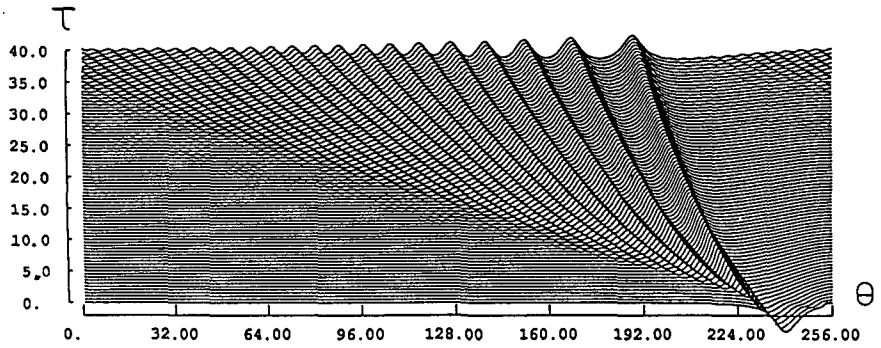

FIG. 3. As in Fig. 2, but $a_0 = -0.3$.

set $\beta_0 = 10$, and consider the numerical integration of (2.47a) for a range of values of a_0. A typical result is shown in Fig. 5 for $a_0 = 0.3$. This should be compared with Fig. 2 which shows the result for the same parameter setting except that $\lambda = 0$. The results are qualitatively similar; as in Fig. 2, a well-defined main wave has emerged, accompanied by the formation of a secondary wave. However, a third wave could not be identified, possibly because the integration was terminated at $\tau = 20$ (in contrast to $\tau = 35$ in Fig. 2). The main wave is slightly smaller in amplitude, slightly slower and slightly wider, than the corresponding wave in Fig. 2.

3. Waves on a potential vorticity front

a. Theory

In this section we shall consider the waves that form on the interface which separates two regions of constant potential vorticity. As we foreshadowed in section 2a one of our aims here is to construct a model that takes into account the dynamical effect of particle paths which may cross the shelf-break. The analysis is analogous to the long-wave limit of the work of Stern and Pratt (1985) and Pratt and Stern (1986), who considered similar problems to that being discussed here but

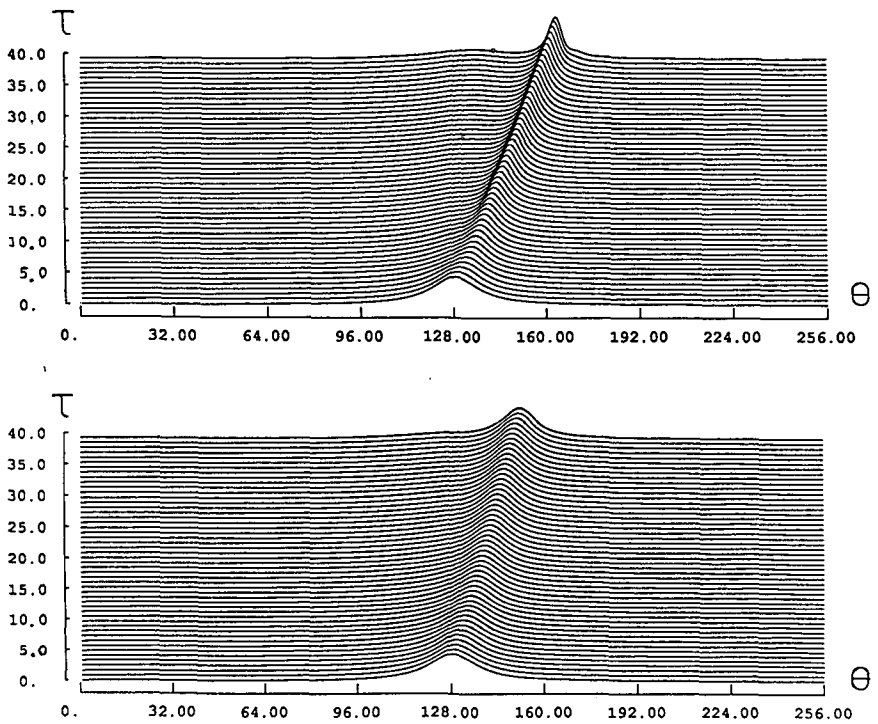

FIG. 4. As in Fig. 2, but the parameter setting is $\delta = 2.5$, $\lambda = 0$, $\gamma_2 = 10$ and (a) $\gamma_3 = 20$, (b) $\gamma_3 = -20$. The initial condition is (2.49) with $a_0 = 0.2$ and $\beta_0 = 10$.

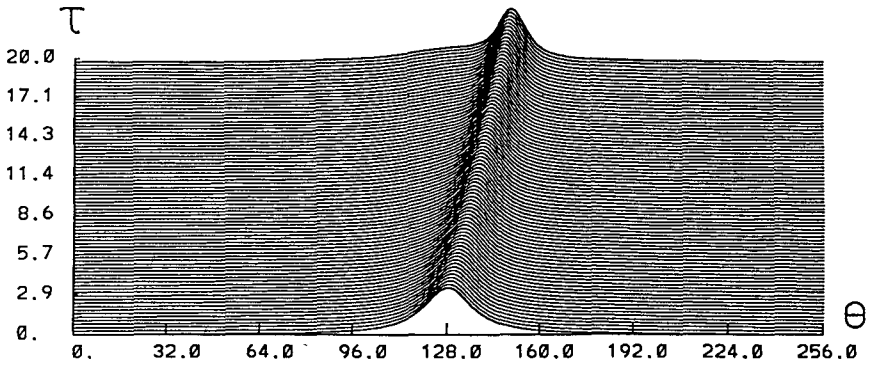

FIG. 5. As in Fig. 2, but the parameter setting is $\delta = 2.5$, $\lambda = 2.5$, $\gamma_2 = 10$, $\gamma_3 = 0$. The initial condition is (2.49) with $a_0 = 0.3$ and $\beta_0 = 10$.

without the effect of the bottom topography. Here we shall suppose that the depth $h(\xi)$ is given by

$$\frac{1}{h(\xi)} = H_0(\xi), \tag{3.1}$$

where $H_0(\xi)$ is everywhere continuous, finite and tends to h_0^{-1} as $\xi \to \infty$. Specific forms for $H_0(\xi)$ will be defined later. However, it is useful to define $\xi = 1$ as the shelf-break, where we anticipate that h will be effectively equal to h_0 in $\xi > 1$.

Suppose that $\xi = L(y, t)$ denotes the interface between two regions of constant vorticity, where $L > 0$ and $L \to 1$ as $y \to -\infty$. Thus we put

$$Q = Q_1, \quad 0 < \xi < L, \tag{3.2a}$$

$$Q = Q_0, \quad \xi > L, \tag{3.2b}$$

where $Q_0 = f/h_0$, and $Q_0 \neq Q_1$. This expression for the potential vorticity satisfies the potential vorticity equation (1.2a) for all points, except those on the interface, where the following boundary conditions must hold,

$$\psi, \psi_\xi \quad \text{continuous at} \quad \xi = L, \tag{3.3a}$$

$$L_t = \frac{\partial}{\partial y}\{\psi(L, y, t)\}. \tag{3.3b}$$

These boundary conditions are derived in Appendix B. In addition the boundary conditions (1.3a, b) must be satisfied at the coast, and at infinity respectively. To describe long waves we introduce the slow variables

$$Y = \epsilon y, \quad T = \epsilon t, \tag{3.4}$$

where ϵ is a small parameter.

1) SHELF REGION

This is the region $0 < \xi < L$. Using (3.2a) and (3.4) we see that (1.7b) becomes

$$fH_0 - \psi_{\xi\xi} - \epsilon^2 H_0^2 \psi_{YY} = Q_1, \tag{3.5}$$

while the boundary condition (1.3a) will be satisfied by choosing $\psi = 0$ at $\xi = 0$. Omitting the term of $O(\epsilon^2)$, the solution of (3.5) is

$$\psi = -V(Y, T)\xi - \tfrac{1}{2} Q_1 \xi^2 + fI(\xi), \tag{3.6a}$$

where

$$I(\xi) = \int_0^\xi d\xi' \int_0^{\xi'} H_0(\xi'')d\xi''. \tag{3.6b}$$

Here $V(Y, T)$ is undetermined at this stage, and represents a longshore current at the coast (see 1.7a). The boundary condition (3.3b) now becomes [to $O(\epsilon^2)$],

$$L_T = \frac{\partial}{\partial Y}\left\{-VL - \frac{1}{2} Q_1 L^2 + fI(L)\right\}. \tag{3.7}$$

This provides one equation linking L and V. A second equation is needed, and this will be obtained from the boundary conditions (3.3a) and the solution in the ocean region.

2) OCEAN REGION

This is the region $\xi > L$. As we intimated in section 2 [see the first paragraph of subsection a(1)] strictly speaking it is necessary to use an intermediate matching to describe the transition from the shelf region where ξ scales with 1 to the outer ocean region where ξ scales with ϵ^{-1}. However, for simplicity, we describe here an alternative procedure which sub-divides the ocean region into two parts, $L < \xi < \xi_0$ and $\xi > \xi_0$. Here ξ_0 scales with 1 and is chosen so that $L < \xi_0$ for all Y, T (e.g., a simple choice could be $\xi_0 = 2$, and then the solution must satisfy $0 < L < 2$). In $L < \xi < \xi_0$, ξ scales with 1, but in $\xi > \xi_0$, ξ will scale with ϵ^{-1}. In effect the intermediate matching is compressed into the location $\xi = \xi_0$, where we require ψ, ψ_ξ to be continuous. For this procedure to be effective it is essential that the final result, the evolution equation for L, should not depend on ξ_0, and indeed we find this to be the case.

For $L < \xi < \xi_0$ we proceed similarly to subsection 1. Thus (1.7b) becomes

$$fH_0 - \psi_{\xi\xi} - \epsilon^2 H_0^2 \psi_{YY} = Q_0, \tag{3.8}$$

where we recall that $Q_0 = f/h_0$. Omitting the term of $O(\epsilon^2)$ the solution of (3.8) is

$$\psi = C - W\xi - \tfrac{1}{2} Q_0 \xi^2 + fI(\xi), \tag{3.9}$$

where C, W are functions of Y, T, and are undetermined at this stage. They are found by imposing the continuity conditions (3.3a). We then find that

$$\psi = -V\xi + (Q_1 - Q_0)\left(\tfrac{1}{2} L^2 - L\xi\right) - \tfrac{1}{2} Q_0 \xi^2 + fI(\xi). \tag{3.10}$$

For $\xi > \xi_0$ we proceed similarly to the analysis of the ocean region in section 2a(1). Thus we put

$$\phi = \epsilon(\xi - \xi_0) \tag{3.11}$$

and since h is effectively equal to h_0 here, we see that (3.8) becomes

$$\psi_{\phi\phi} + \frac{1}{h_0^2} \psi_{YY} = 0 \tag{3.12}$$

Using the boundary condition (3.1b) the solution of (3.12) is

$$\psi = C_0 - W_0(\xi - \xi_0) + \Psi(\phi, Y, T), \tag{3.13a}$$

where

$$\Psi = \frac{1}{2\pi} \int_{-\infty}^{\infty} \mathcal{F}(\Psi(\phi = 0)) \exp\left(ilY - \frac{|l|\phi}{h_0}\right) dl. \tag{3.13b}$$

We recall that the Fourier transform $\mathcal{F}(\cdot)$ is defined by (2.18b). Here C_0 and W_0 are constants, and the first two terms in (3.13a) are needed to allow for a uniform longshore current (i.e. W_0) in the ocean region. We note that

$$\Psi_\phi(\phi = 0) = \frac{1}{h_0} \mathcal{B}(M) \tag{3.14a}$$

where

$$M(Y, T) = \Psi(\phi = 0), \tag{3.14b}$$

and the operator $\mathcal{B}(\cdot)$ is defined by (2.19b). Next we impose the conditions that ψ, ψ_ξ are continuous at $\xi = \xi_0$, and we note that the main reason for introducing ξ_0 is so that the Fourier transforms in (3.13b) and (3.14a) can be matched across a straight line, rather than the variable interface $\xi = L$. We find that

$$-V\xi_0 + (Q_1 - Q_0)\left(\tfrac{1}{2} L^2 - L\xi_0\right) - \tfrac{1}{2} Q_0 \xi_0^2 + fI(\xi_0) = C_0 + M, \tag{3.15a}$$

$$-V - (Q_1 - Q_0)L - Q_0\xi_0 + fI'(\xi_0) = -W_0 + \frac{\epsilon}{h_0} \mathcal{B}(M). \tag{3.15b}$$

This pair of equations determines M and V in terms of L and hence closes the evolution equation (3.7).

3) Results

To proceed, we first note that since h is effectively equal to h_0 for $\xi > 1$, we may deduce from (3.6b) that

$$I(\xi) = \frac{\xi^2}{2h_0} + I_1\xi + I_2, \quad \text{for} \quad \xi > 1, \tag{3.16a}$$

where

$$I_1 = \int_0^\infty \left\{H_0(\xi) - \frac{1}{h_0}\right\} d\xi, \tag{3.16b}$$

$$I_2 = -\int_0^\infty d\xi \int_\xi^\infty \left\{H_0(\xi') - \frac{1}{h_0}\right\} d\xi'. \tag{3.16c}$$

Next we suppose that $L \to 1$, $V \to V_0$ and $M \to 0$ as $Y \to -\infty$. Taking this limit in (3.15a, b) we find that

$$C_0 = -\xi_0 W_0 + \tfrac{1}{2}(Q_1 - Q_0) + fI_2, \tag{3.17a}$$

$$W_0 = V_0 + (Q_1 - Q_0) - fI_1. \tag{3.17b}$$

Then using the expressions (3.16a–c) and (3.17a, b), we find that (3.15a, b) simplify to

$$M = \tfrac{1}{2}(Q_1 - Q_0)(L^2 - 1) + O(\epsilon), \tag{3.18a}$$

$$V - V_0 = -(Q_1 - Q_0)(L - 1) - \frac{\epsilon}{h_0} \mathcal{B}(M), \tag{3.18b}$$

which are the required relations expressing M and V in terms of L. The $O(\epsilon)$ term in (3.18a) will not be needed as it gives only an $O(\epsilon^2)$ correction to (3.18b), and we have already rejected terms which are $O(\epsilon^2)$ in (3.5) and (3.8). Finally the expressions (3.18a) are substituted into (3.7) to give

$$L_T = \frac{\partial}{\partial Y}\left\{-V_0 L + (Q_1 - Q_0)L(L - 1) - \tfrac{1}{2} Q_1 L^2 + fI(L) + \frac{\epsilon L}{h_0} \mathcal{B}(M)\right\}, \tag{3.19a}$$

where

$$M = \tfrac{1}{2}(Q_1 - Q_0)(L^2 - 1). \tag{3.19b}$$

This equation can be further simplified by writing (3.6b) in the form (compare (3.16a))

$$I(\xi) = \frac{\xi^2}{2h_0} + I_1\xi + I_2 + \int_\xi^\infty J(\xi')d\xi' \tag{3.20a}$$

where

$$J(\xi) = \int_{\xi}^{\infty} \left\{ H_0(\xi) - \frac{1}{h_0} \right\} d\xi. \tag{3.20b}$$

On substituting (3.20a) into (3.19a) we obtain

$$L_T = (-V_0 + fI_1)L_Y + (Q_1 - Q_0)(L-1)L_Y - fJ(L)L_Y + \left\{ \frac{\epsilon L}{h_0} \mathcal{B}(M) \right\}_Y. \tag{3.21}$$

With M given by (3.19b), this is a nonlinear evolution equation for L in which the nonlinear terms derive both from the vorticity discontinuity $(Q_1 - Q_0)$, and the topographic term $J(L)$ (3.20b), while the dispersive term involving the operator $\mathcal{B}(\cdot)$ is also here nonlinear. The error term in (3.21) is $O(\epsilon^2)$.

To assist in the integration of (3.21) we now introduce some further changes of variable and rescaling. We put

$$L = 1 + A, \tag{3.22a}$$

$$\theta = Y - (V_0 - fI_1)T, \quad \tau = |Q_1 - Q_0|T, \tag{3.22b}$$

$$J(L) = -(Q_1 - Q_0)K(L). \tag{3.22c}$$

Note here that since h is effectively equal to h_0 for $\xi > 1$, $J(L) = 0$ for $L \geq 1$, and so $V_0 - fI$, is the speed of an infinitesimal long wave on the interface. Using (3.22a–c), (3.21) becomes

$$\mp A_\tau + AA_\theta + fK(1+A)A_\theta + \left\{ \frac{\epsilon}{h_0}(1+A)\mathcal{B}\left(A + \frac{1}{2}A^2\right) \right\}_\theta = 0, \tag{3.23}$$

where the alternate signs refer to the cases $Q_1 \gtrless Q_0$ respectively. Unlike the case considered in section 2 the dispersive term here remains of $O(\epsilon)$ but is, of course, needed to oppose wave-steepening. We shall seek solutions of (3.23) such that $A \to 0$ as $\theta \to \pm\infty$ and subject to the restriction that $A > -1$ (corresponding to $L > 0$). In the limit $A \to 0$, (3.23) reduces to the deep-fluid internal solitary-wave equation derived by Benjamin (1967) and Davis and Acrivos (1967), which we have denoted here as the BDA equation. In the absence of the topographic term [i.e., $K(L) \equiv 0$] it agrees in this limit with the analysis of Stern and Pratt (1985) of vorticity fronts. The fully nonlinear form (3.23) has some similarities with the small-curvature, finite-amplitude equation of Pratt and Stern (1986) (see also Pratt 1988) for potential vorticity fronts in the absence of topography. In considering (3.23) we shall always assume that the coefficient of A_τ is $+1$ corresponding to $Q_1 < Q_0$. For the case $Q_1 > Q_0$, the transformation $\theta \to -\theta$ reverses the sign of the coefficient of A_τ, and leads to the same equation. Finally in order to obtain numerical solutions to (3.23) we must give an explicit form for $K(L)$. For simplicity we choose $H_0(\xi) = D + B\xi$, $0 < \xi < 1$, which is the same depth profile used in section 2 [see (2.3b)]. We then find that

$$fK(1+A) = \tfrac{1}{2}\gamma A^2 H(-A), \tag{3.24a}$$

where

$$\gamma = fB(Q_1 - Q_0)^{-1}. \tag{3.24b}$$

Here $H(\cdot)$ is the Heaviside function.

b. Numerical results

Equation (3.23) was integrated numerically using a pseudospectral scheme analogous to that developed by Fornberg and Whitham (1978) for the Korteweg-de Vries equation, and similar to that used for (2.47a) in section 2b, although now, of course, without the complications caused there by the integral terms. In the small-amplitude limit $A \to 0$, (3.23) reduces to the BDA equation.

$$A_\tau + AA_\theta + \frac{\epsilon}{h_0}\mathcal{B}(A_\theta) = 0, \tag{3.25}$$

which has the solitary wave solution [cf. (2.45a, b)]

$$A = \frac{a}{1 + [(\theta - \omega\tau)/\beta]^2}, \tag{3.26a}$$

where

$$w = \frac{a}{4} = \frac{\epsilon}{h_0\beta}. \tag{3.26b}$$

In our discussion of (3.23) we shall use this result as a benchmark, and hence use the initial condition [cf. (2.49)]

$$A(\tau = 0) = \frac{a_0}{1 + \{(\theta - \theta_0)/\beta_0\}^2}. \tag{3.27}$$

For the BDA equation (3.25), with $a_0\beta_0 = 4\epsilon/h_0$ this will produce the solitary wave (3.26a) with speed w given by (3.26b). In choosing numerical values for the coefficients γ and ϵ/h_0, we note that ϵ/h_0 is disposable, even though ϵ is a small parameter, since a rescaling of the variables τ and θ allows it to be chosen arbitrarily. However γ is not disposable. We choose $\epsilon/h_0 = 0.25$, and either set $\gamma = 0$ corresponding to the effective absence of any topographic effects, or set $\gamma = \pm 1$, the alternate signs corresponding to a northern or southern hemisphere scenario respectively (see (3.24b) and recall that we have chosen $Q_1 < Q_0$).

First we put $\gamma = 1$ and consider the numerical integration of (3.23) with $\beta_0 = 10$ for a range of values of a_0 (0.1 to 0.5). A typical result is shown in Fig. 6 for $a_0 = 0.3$. In general the results are similar to the analogous results for the BDA equation (3.25) [and also to our results for the numerical integration of

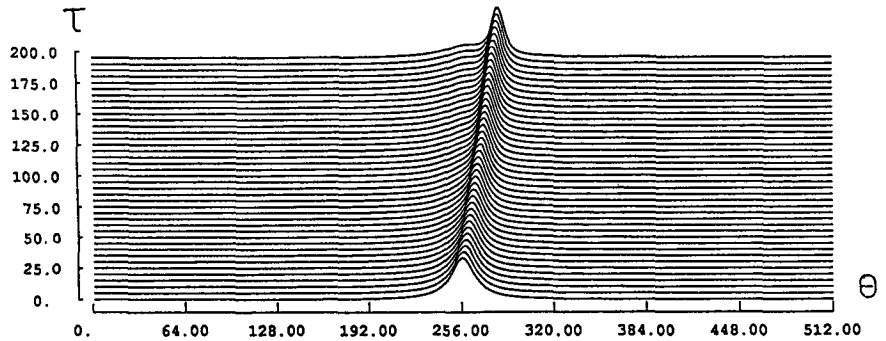

FIG. 6. Results for the numerical integration of the nonlinear evolution equation (3.23). The parameter setting is $\epsilon/h_0 = 0.25$, $\gamma = 1$. The initial condition is (3.27) with $a_0 = 0.3$ and $\beta_0 = 10$.

(2.47a)]. Note that for $a_0 = 0.1$, $a_0\beta_0 = 4\epsilon/h_0$ thus satisfying the condition (3.26) for a solitary wave solution of the BDA equation (3.25). For this case the numerical integration indeed produced a single solitary wave. As a_0 is increased, more waves are produced. For the case $a_0 = 0.3$ we see from Fig. 6 that in addition to the main wave, a secondary wave is forming; although it cannot be seen on the scale of the figure, a third wave is also forming together with some trailing oscillations. These features are qualitatively similar to the behavior to be expected from the BDA equation (3.25), which for this particular initial condition would be expected to produce three solitary waves. To compare the main wave produced with the solitary wave solution of the BDA equation (3.25), the numerical integrations were repeated with $a_0\beta_0 = 1$ (i.e., $a_0\beta_0 = 4\epsilon/h_0$) and the same range of values of a_0. In Fig. 7 we plot the numerically determined speed w, width β as functions of the amplitude a. Here 2β is defined to be the width of the wave when the amplitude is $\frac{1}{2}a$, where a is the amplitude at the crest. Note that there is some uncertainty in determining w and β, as the waves were not quite steady throughout the time of the numerical integration. Nevertheless, the results give some quantitative indication of how the speed w and width β vary with amplitude a. In Fig. 7 we compare these numerical results with the corresponding predictions (3.26b) of the BDA equation. We see that the waves are wider, for a given amplitude, than the corresponding BDA solitary wave, with the trend increasing as the amplitude increases. However, the speeds are very close to those of the corresponding BDA solitary waves. Finally we note that with the choice $a_0 > 0$, the wave field produced has $A > 0$ except in the region of the trailing oscillations, which were generally of very small amplitude. Hence the topographic term (3.24a) whose coefficient is γ, makes only a very small contribution, since it is nonzero only when $A < 0$. Thus we would expect the choice of γ, either positive or negative, to have very little effect on the solutions when the initial condition has $a_0 > 0$. Indeed, repeating the numerical integrations with the same initial conditions described above, but putting $\gamma = 0$, gave results that were numerically indistinguishable from those for $\gamma = 1$.

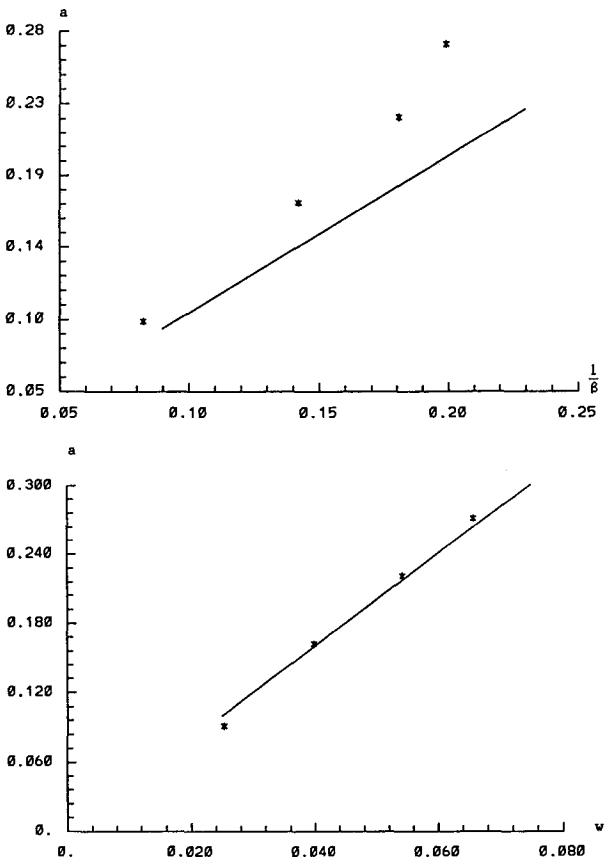

FIG. 7. Results for the amplitude, speed and width of the waves found by numerical integration of (3.23). (a) A plot of the amplitude a as a function of β^{-1}, where β is the width. (b) A plot of the amplitude a as a function of the speed w. The numerical results are denoted by ($\times$), and the corresponding results (3.25) for the BDA equation are denoted by the solid straight line.

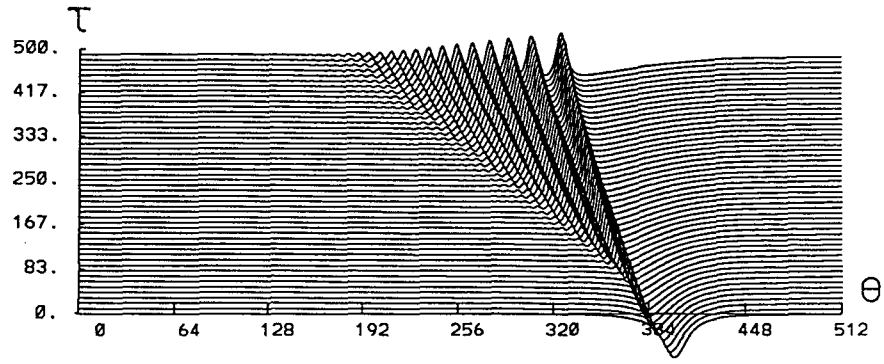

FIG. 8. As in Fig. 6, but $\gamma = -1$ and $a_0 = -0.3$.

Next we put $\gamma = 1$, $\beta_0 = 10$ but choose $a_0 < 0$ in the initial condition (3.27). A typical result for $a_0 = -0.3$ is shown in Fig. 8. The wave field now consists of an oscillatory wavetrain propagating in the negative θ-direction. Again these features are typical of the behavior to be expected from the BDA equation (3.25) for this negative initial condition. Since, for $a_0 < 0$, the choice of γ is now significant [see (3.24a)], the numerical integrations were repeated with $\gamma = -1$. The results are generally similar to the case $\gamma = 1$, but the evolving wave field is larger in amplitude and extent, and is faster in its development. The reason for this is that the nonlinear term in (3.23) is, with $A < 0$, $A(1 + \frac{1}{2}\gamma A)A_\theta$. Hence the nonlinearity is increased (decreased) when $\gamma < 0$ (>0).

Finally we note that in the theoretical development of this section we chose to place the shelf-break at $\xi = 1$, which is the same location as the vorticity interface as $Y \to \infty$ (i.e. $L \to 1$ as $Y \to \infty$). This was done for simplicity, and we now explore the consequences of relaxing this condition and supposing instead that the shelf-break is at $\xi = \xi_1$. Then the theoretical development of section 3a is largely unchanged, and (3.23) is obtained as before. If we again choose $H_0(\xi) = D + B\xi$, but now this holds for $0 < \xi < \xi_1$, we find that, in place of (3.24a),

$$fK(1 + A) = \frac{1}{2}\gamma(A_1 - A)^2 H(A_1 - A), \quad (3.28)$$

where γ is again given by (3.24b), and $A_1 = \xi_1 - 1$. If $A_1 < 0$ and we use the initial condition (3.27) with $a_0 > 0$, then the wave field produced has $A > 0$ except for some very small amplitude trailing oscillations. In this case the topographic term (3.28) does not contribute to the solution for any value of γ. Only if $A_1 > 0$ will the topographic term (3.28) have some influence on the solution for the case when $a_0 > 0$. In Fig. 9 we show the result of the numerical integration of (3.23) for the initial condition (3.27) with $a_0 = 0.4$ and $\beta_0 = 10$; we set $A_1 = 0.2$ and $\gamma = \pm 5$. The evolving wave field is qualitatively similar to the case $\gamma = 0$, although the main wave to emerge is larger in amplitude, but slower. Further, for the case $\gamma = -5$ the main wave is larger in amplitude and slower in speed than for the case $\gamma = 5$. The reasons for this behaviour can be sought by considering the impact of the topographic term (3.28) on the nonlinear term AA_θ. Note that the topographic term equals $\frac{1}{2}\gamma A_1^2$ when $A = 0$ (since here

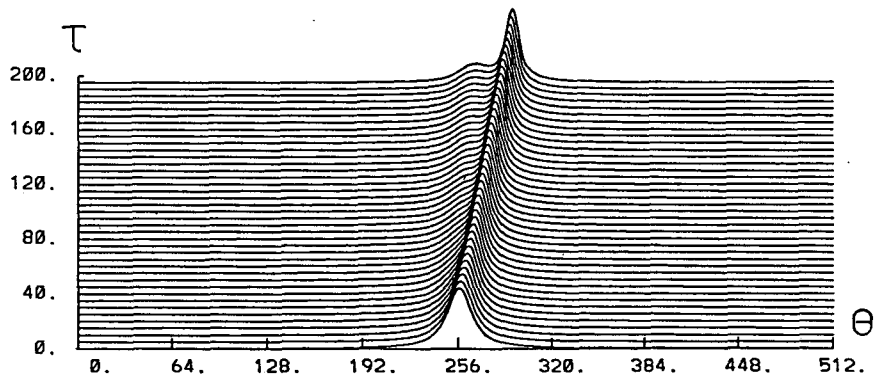

FIG. 9. Results for the numerical integration of the nonlinear evolution equation (3.23), when adapted by (3.28). The parameter setting is $\epsilon/h_0 = 0.25$, $A_1 = 0.2$ and (a) $\gamma = 5$, (b) $\gamma = -5$. The initial condition is (3.27) with $a_0 = 0.4$ and $\beta_0 = 10$.

$A_1 > 0$), and this term can be interpreted as a contribution to the speed of a wave. On this basis we would expect waves for $\gamma > 0$ to be faster than waves for $\gamma < 0$. However, relative to this level of $\frac{1}{2}\gamma A_1^2$, the topographic term (3.28) enhances the nonlinearity when $\gamma < 0$, and reduces it when $\gamma > 0$; this tendency runs counter to the effect of the term $\frac{1}{2}\gamma A_1^2$ when considered alone, since an increase in nonlinearity generally implies an increase in speed. Thus, it is possible, as our numerical results show, for the topographic term (3.28) to have the effects described above.

4. Summary

In this paper we have described two models of coastal currents which allow us to obtain fully nonlinear wavelike solutions in the limit of long waves. The first model, described in section 2, uses a particular choice of shelf topography (2.3b) for which, at leading order, the potential vorticity is a linear function of the transport streamfunction [see (2.21) and (2.22)]. This device enables us to derive the nonlinear evolution equation (2.47a) for long waves without any restriction to small-amplitude waves, except for the constraint (2.36). Topographic and shear perturbations contribute to the nonlinearity of the equation while dispersion is derived from the interaction of the wave field with the flow in the adjoining deep ocean.

The second model, described in section 3, describes the waves that form at a vorticity interface separating two regions of constant potential vorticity. For long waves this allows for a relatively simple description of the flow on the shelf, and the result is the nonlinear evolution (3.23) for which the dispersive term is again provided by the effect of the adjoining deep ocean. For this model the choice of shelf topography is not so crucial, and affects only the form of the nonlinear terms.

For both model nonlinear evolution equations we have presented some numerical results that explore the dependence of the solutions on various parameters, including those which occur in the equations themselves as well as those occurring in the initial conditions. In qualitative terms the wave fields produced are similar for the two model equations, and also similar to the waves described by the BDA equation, which is the weakly nonlinear limit for both evolution equations. This is reassuring as it implies that the BDA equation, which is exactly integrable, can be used to study nonlinear long waves for situations where the present fully nonlinear equations do not apply. Indeed the BDA equation is the canonical evolution equation for weakly nonlinear long waves in the continental shelf waveguide (Smith 1975).

There are a number of areas where the present theories could be improved. For instance, inclusion of the effects of density stratification and bottom friction is necessary if model calculations are to be of practical quantitative utility. However, more pertinent is the need to relax the long-wave hypothesis, and develop models for fully nonlinear wave fields which allow the flow to develop on all length scales, including potentially very short scales. In this respect the vorticity interface model of section 3 clearly can be extended in this way, and the result would be a nonlinear integral equation which can be solved by the method of contour dynamics. The model proposed here is similar to that developed by Pratt and Stern (1986). Work on this approach is proceeding.

Acknowledgments. One of us (Yi) acknowledges support from Grant 880610 from the Dept. of Industry, Technology and Commerce (Australia) under the China–Australia Science and Technology Program.

APPENDIX A

Boundary Conditions at a Discontinuity in Depth

Suppose there is discontinuity in depth at $x = x_s$ so that $h \to h_s$ as $x \to x_s-$ and $h \to h_0$ as $x \to x_s+$ (see Fig. 1). Assuming that u, v and ζ are likewise discontinuous at $x = x_s$, we derive here the appropriate discontinuity conditions. To do this, we employ a limiting procedure in which we suppose that h is continuous over an interval of width δ centered on $x = x_s$, and varies from h_s for $x < x_s - \delta$ to h_0 for $x > x_s + \delta$. Consequently h_x scales with δ^{-1} as x passes through $x - x_s$. Likewise the derivatives of u, v and ζ with respect to x will scale with δ^{-1}. Each equation (1.1a–c) is then integrated with respect to x over the interval $x_s - \delta < x < x_s + \delta$. We then take the limit $\delta \to 0$. Applying this procedure to (1.1c) we find that

$$[hu] = 0 \tag{A1}$$

where $[\cdot]$ denotes the discontinuity across $x = x_s$. Using (1.4) we see that this is equivalent to the continuity of ψ at $x = x_s$, where we assume that ψ is continuous as $y \to \infty$. The condition (A1) reflects the continuity of the onshore mass flux.

Applying the same procedure to (1.1a, b) we find that

$$\left[\zeta + \frac{1}{2}u^2\right] = 0, \tag{A2a}$$

$$[huv] = 0. \tag{A2b}$$

Here (A2b) expresses the continuity of the x-component of the longshore momentum flux. Since hu is continuous, (A2b) is equivalent to

$$[v] = 0 \tag{A3}$$

where we have assumed that hu is not identically zero at the shelf-break. From (1.7a) we see that (A3) is equivalent to the continuity of ψ_ξ. Thus (A1) and (A3) determine the behavior of u and v respectively, while (A2a) then gives the discontinuity of ζ. It is noteworthy

here that the discontinuity conditions (A1) and (A3) differ from those which are usually applied in linear problems. Indeed, the corresponding derivation in a linear problem leads to (A1) and the linearized form of (A2a), namely, that ζ is continuous.

It should be noted here that in the region where the depth varies rapidly significant vertical velocities will be generated, and these may be of sufficient magnitude to invalidate the barotropic, shallow-water equations (1.1a–c). Indeed the vertical velocity scales with h_1/L_1 relative to the horizontal velocities, where we recall that h_1 is a typical vertical dimension, and L_1 is a typical horizontal length scale. However, in the regions where the depth varies rapidly the vertical velocity will scale with $h_1/\delta L_1$, and hence the preceeding derivation requires that $h_1/L_1 \ll \delta \ll 1$. This condition is likely to be met in many practical situations. However a derivation, similar to the above, which allows δ to be comparable with h_1/L_1, has also been carried out, and again leads to (A1) and (A3).

APPENDIX B

Boundary Condition at a Potential Vorticity Front

Suppose that $\xi = L(y, t)$ denotes a curve across which the potential vorticity Q is discontinuous. In deriving the boundary conditions we find it convenient to revert here to the original $(x - y)-$ coordinates, and so we let the interface be given by [see (1.6)]

$$x = \hat{L}(y, t), \quad \text{where} \quad L = \int_0^{\hat{L}} h(x')dx'. \tag{B1}$$

Then since the interface is a material curve, the following kinematic condition must hold

$$u = \hat{L}_t + v\hat{L}_y, \quad \text{on} \quad x = \hat{L} \tag{B2a}$$

or

$$hu = L_t + vL_y, \quad \text{on} \quad \xi = L. \tag{B2b}$$

Introducing the streamfunction ψ [see (1.4) and (1.7a)], (B2a, b) becomes

$$L_t = \frac{\partial}{\partial y}\{\psi(L, y, t)\}. \tag{B3}$$

It follows from (B2) that ψ is continuous across $\xi = L$, where we assume that ψ is a continuous function of ξ as $y \to -\infty$.

The remaining boundary condition is the continuity of the pressure, ζ. However, to be useful in the present context this condition must be translated into a condition on ψ. To achieve this we first use the equations of motion (1.1a, b) and (B2a) to show that

$$\frac{\partial}{\partial y}\{\zeta(\hat{L}, y, t)\} = -f\hat{L}_t - \frac{dv}{dt} - \hat{L}_y\frac{du}{dt}, \quad \text{on} \quad x = \hat{L}. \tag{B4}$$

But, using (B2a) it may be shown that

$$\frac{d}{dt}(u, v) = \left(\frac{\partial}{\partial t} + v\frac{\partial}{\partial y}\right)\{(u, v)(\hat{L}, y, t)\}, \quad \text{on} \quad x = \hat{L}. \tag{B5}$$

On substituting (B5) into (B4), using (B2a) and letting $[\zeta]$, $[v]$ denote the discontinuity in ζ, v respectively at the interface, we may show that

$$\frac{\partial}{\partial y}[\zeta] = -\frac{\partial}{\partial t}\{(1 + \hat{L}_y^2)[v]\} - \frac{\partial}{\partial y}\left\{(1 + \hat{L}_y^2)\left[\frac{1}{2}v^2\right]\right\}. \tag{B6}$$

Hence, if $[\zeta] = 0$, it follows that $[v]$ is conserved along the interface, and assuming that $[v] = 0$ as $y \to -\infty$, we have shown that $[v] = 0$ on $x = \hat{L}$. Recalling (1.7a) we see that this is equivalent to ψ_ξ being continuous across the interface. Also we note from (B6) that the converse is true, namely, if $[v] = 0$, then $[\zeta] = 0$.

REFERENCES

Benjamin, T. B., 1967: Internal waves of permanent form in fluids of great depths. *J. Fluid Mech.*, **29,** 559–592.

Craik, A. D. D., 1985: *Wave interactions and fluid flows.* CUP, 322 p.

Davis, R. E., and A. Acrivos, 1967: Solitary internal waves in deep water. *J. Fluid Mech.*, **29,** 593–607.

Fornberg, B., and G. B. Whitham, 1978: A numerical and theoretical study of certain nonlinear wave phenomena. *Phil. Trans. Roy. Soc.*, **A289,** 373–404.

Kakutani, T., and N. Yamasaki, 1978: Solitary waves on a two-layer fluid. *J. Phys. Soc. Japan,* **45,** 674–679.

Miles, J. W., 1979: On internal solitary waves. *Tellus,* **31,** 456–462.

Pedlosky, J., 1986: *Geophysical Fluid Dynamics,* second edition. Springer, 710 pp.

Pratt, L. J., 1988: Meandering and eddy detachment according to a simple (looking) path equation. *J. Phys. Oceanogr.*, **18,** 1627–1640.

——, and M. E. Stern, 1986: Dynamics of potential vorticity fronts and eddy detachment. *J. Phys. Ocean.*, **16,** 1101–1120.

Smith, R., 1975: Nonlinear Kelvin and continental-shelf waves. *J. Fluid Mech.*, **52,** 379–391.

Stern, M. E., 1980: Geostrophic fronts, bores, breaking and blocking waves. *J. Fluid Mech.*, **99,** 687–703.

——, and L. J. Pratt, 1985: Dynamics of vorticity fronts. *J. Fluid Mech.*, **161,** 513–532.

Warn, T., 1983: The evolution of finite amplitude solitary Rossby waves on a weak shear. *Stud. Appl. Math.*, **69,** 127–133.

Yi, Z. and T. Warn, 1987: A numerical method for solving the evolution equation of solitary Rossby waves on a weak shear. *Adv. Atmos. Sci.*, **4,** 43–54.